

## Supplementary Information

### **Nonvolatile electrical control of valley splitting by ferroelectric polarization switching in two-dimensional $\text{AgBiP}_2\text{S}_6/\text{CrBr}_3$ multiferroic heterostructure**

Dongxue Zhang, Yifan Zhang, Baozeng Zhou\*

*Tianjin Key Laboratory of Film Electronic & Communicate Devices, School of Integrated Circuit Science and Engineering, Tianjin University of Technology, Tianjin 300384, China*

\*Corresponding Authors

[baozeng@tju.edu.cn](mailto:baozeng@tju.edu.cn) (B. Zhou)

**Table S1.** Interlayer Distances  $d_i$  (Å) between AgBiP<sub>2</sub>S<sub>6</sub> and CrBr<sub>3</sub>, Binding Energy  $E_b$  (meV/atom), Band-Gap  $E_g$  (eV), Total Magnetic Moments  $M_{tot}$  ( $\mu_B$ ), and Energy Difference  $\Delta E_{FM-AFM}$  (meV) for different configurations of the AgBiP<sub>2</sub>S<sub>6</sub>/CrBr<sub>3</sub> vdW heterostructures.

<b>Model</b>		$d_i$ (Å)	$E_b$ (meV/atom)	$E_g$ (eV)	$M_{tot}$ ( $\mu_B$ )	$\Delta E_{FM-AFM}$ (meV)
<b>I</b>	<b>P+</b>	3.15	-188.32	1.19	5.84	-42.86
	<b>P-</b>	3.73	-182.14	1.42	5.84	-41.09
<b>II</b>	<b>P+</b>	3.34	-185.62	1.15	5.84	-41.29
	<b>P-</b>	3.76	-179.47	1.41	5.84	-40.90
<b>III</b>	<b>P+</b>	3.26	-187.60	1.17	5.84	-42.39
	<b>P-</b>	3.80	-179.46	1.39	5.84	-40.70

**Table S2.** The lattice vectors and fractional coordinates of each atom in AgBiP<sub>2</sub>S<sub>6</sub>/CrBr<sub>3</sub> heterostructure with P+ state.

<b>a[Å]</b>	6.3516737391921954	0.0000000338711972	0.0000000000000000
<b>b[Å]</b>	-3.1758368989294152	5.5007107977067626	0.0000000000000000
<b>c[Å]</b>	0.0000000000000000	0.0000000000000000	29.9647006988999998
<b>S</b>	0.9909565350833234	0.6153824755154375	0.4476054072655399
<b>S</b>	0.3846175114845642	0.3755740305678862	0.4476054072655399
<b>S</b>	0.6244259944321126	0.0090435039166768	0.4476054072655399
<b>S</b>	0.3376691530403998	0.0519300521851825	0.3323641611108283
<b>S</b>	0.9480699058148216	0.2857391048552255	0.3323641611108283
<b>S</b>	0.7142609531447792	0.6623308659595973	0.3323641611108283
<b>Br</b>	0.0172715030579112	0.3322965585541545	0.5528608831528239
<b>Br</b>	0.6677034714458490	0.6849749345037568	0.5528608831528239
<b>Br</b>	0.3150250724962477	0.9827284889420868	0.5528608831528239
<b>Br</b>	0.6662523392471248	0.9823661886040973	0.6488545151122515
<b>Br</b>	0.0176338493958982	0.6838861076430283	0.6488545151122515
<b>Br</b>	0.3161138873569764	0.3337477077528752	0.6488545151122515
<b>P</b>	0.6666667060000009	0.3333333380000028	0.3501788018525476
<b>P</b>	0.6666667060000009	0.3333333380000028	0.4257640105547345
<b>Ag</b>	-0.0000000000000000	0.0000000000000000	0.4255378381306612
<b>Bi</b>	0.3333333380000028	0.6666666750000019	0.3798650698726054
<b>Cr</b>	-0.0000000000000000	0.0000000000000000	0.6009813130007060
<b>Cr</b>	0.3333333380000028	0.6666666750000019	0.6007581156644234

**Table S3.** The lattice vectors and fractional coordinates of each atom in AgBiP<sub>2</sub>S<sub>6</sub>/CrBr<sub>3</sub> heterostructure with P– state.

<b>a[Å]</b>	6.3479298765991805	0.0000001374165001	0.0000000000000000
<b>b[Å]</b>	-3.1739650573057689	5.4974684658205364	0.0000000000000000
<b>c[Å]</b>	0.0000000000000000	0.0000000000000000	29.9647006988999998
<b>S</b>	0.9904235723877730	0.6172551697405315	0.3247562426483977
<b>S</b>	0.6268316253527615	0.0095764396122271	0.3247562426483977
<b>S</b>	0.3827448272594640	0.3731684036472387	0.3247562426483977
<b>S</b>	0.3386597105855122	0.0513976193629148	0.4403088212043350
<b>S</b>	0.7127379277773972	0.6613402904144827	0.4403088212043350
<b>S</b>	0.9486023436370893	0.2872621002226043	0.4403088212043350
<b>Br</b>	0.6666200061735178	0.6849993356892514	0.5648679352483319
<b>Br</b>	0.0183794035157319	0.3333799998264828	0.5648679352483319
<b>Br</b>	0.3150006453107513	0.9816205814842700	0.5648679352483319
<b>Br</b>	0.3158648572492148	0.3332540523854736	0.6609852731176955
<b>Br</b>	0.0173891871362584	0.6841351397507880	0.6609852731176955
<b>Br</b>	0.6667459386145294	0.9826108368637442	0.6609852731176955
<b>P</b>	0.6666666750000019	0.3333333380000028	0.4220389154458148
<b>P</b>	0.6666666750000019	0.3333333380000028	0.3463370249089215
<b>Ag</b>	0.0000000000000000	0.0000000000000000	0.3519161150966360
<b>Bi</b>	0.3333333380000028	0.6666667060000009	0.3922070613437507
<b>Cr</b>	0.3333333380000028	0.6666667060000009	0.6130059525070672
<b>Cr</b>	0.0000000000000000	0.0000000000000000	0.6129801780415449

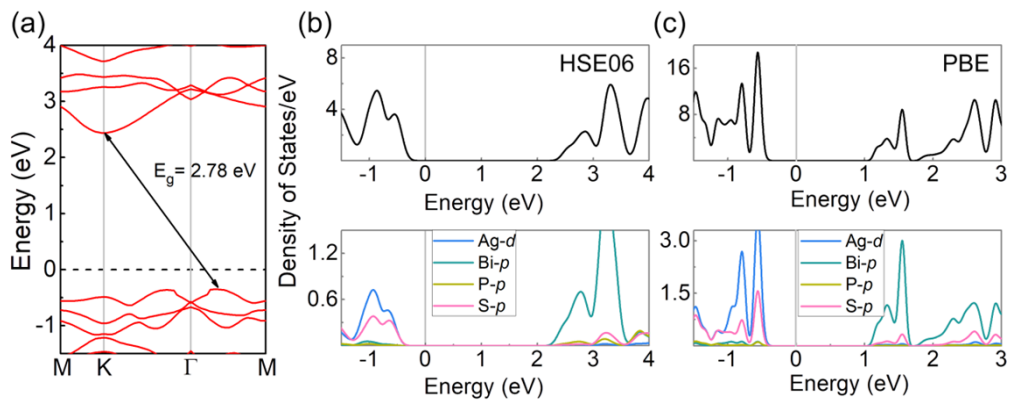


**Fig. S1** (a) Band structure of the monolayer AgBiP<sub>2</sub>S<sub>6</sub> calculated by HSE06 method.

The total DOS and orbital-resolved PDOS for each atom calculated by (b)

HSE06 and (c) PBE method, respectively.

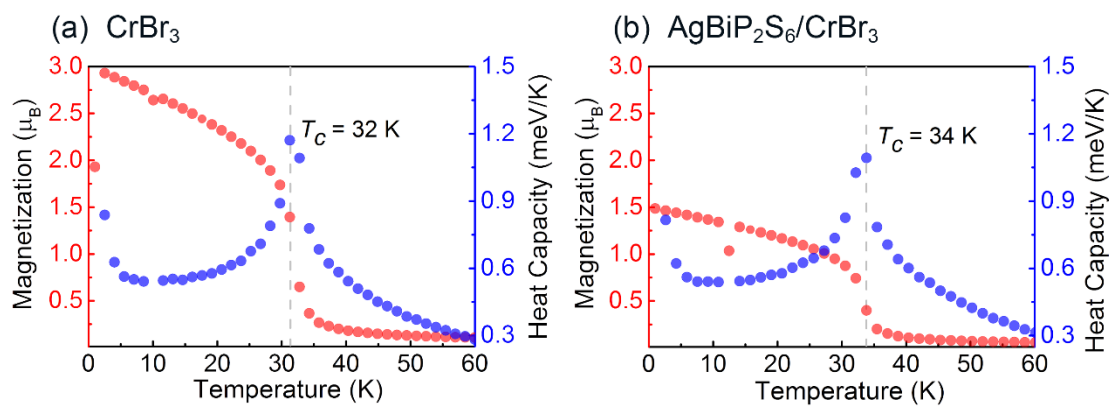


**Fig. S2** The magnetization and heat capacity as functions of temperature for (a)  $\text{CrBr}_3$  monolayer and (b)  $\text{AgBiP}_2\text{S}_6/\text{CrBr}_3$  heterostructure.

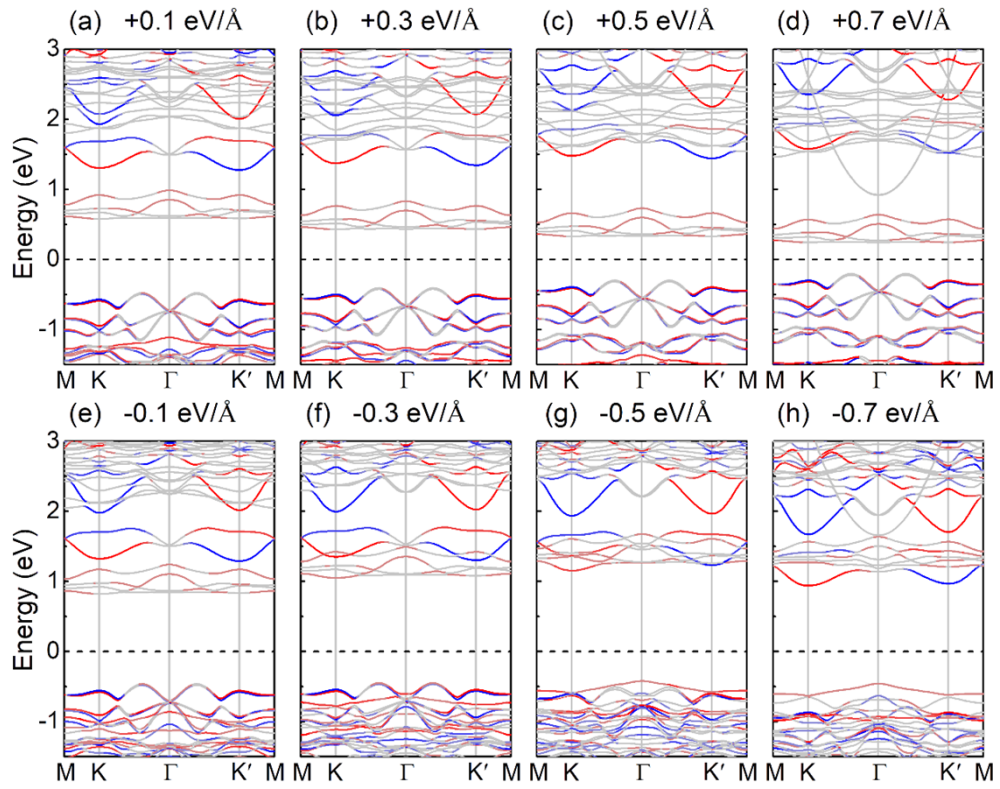


**Fig. S3** Calculated band structures of the  $\text{AgBiP}_2\text{S}_6/\text{CrBr}_3$  heterostructure in the polarized state P+ under different electric field from  $-0.7 \text{ V/\AA}$  to  $+0.7 \text{ V/\AA}$ .

The Fermi level is set to zero.

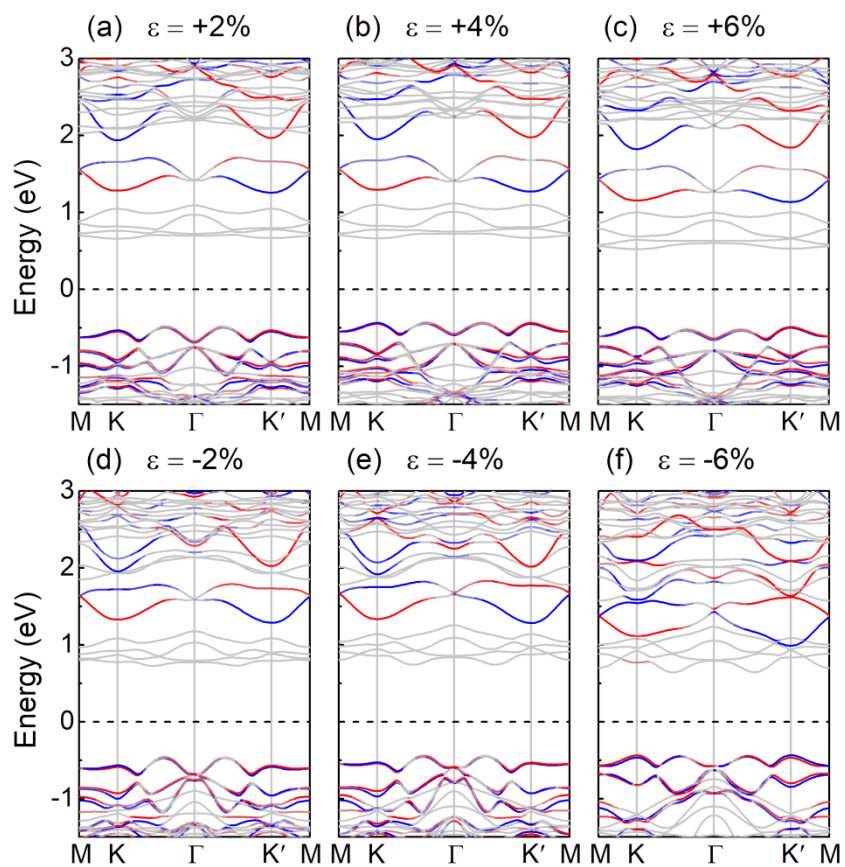


**Fig. S4** Band structures of AgBiP<sub>2</sub>S<sub>6</sub>/CrBr<sub>3</sub> heterostructure in the polarized state P+ under different strain from  $-6\%$  to  $+6\%$ . The Fermi level is set to zero.



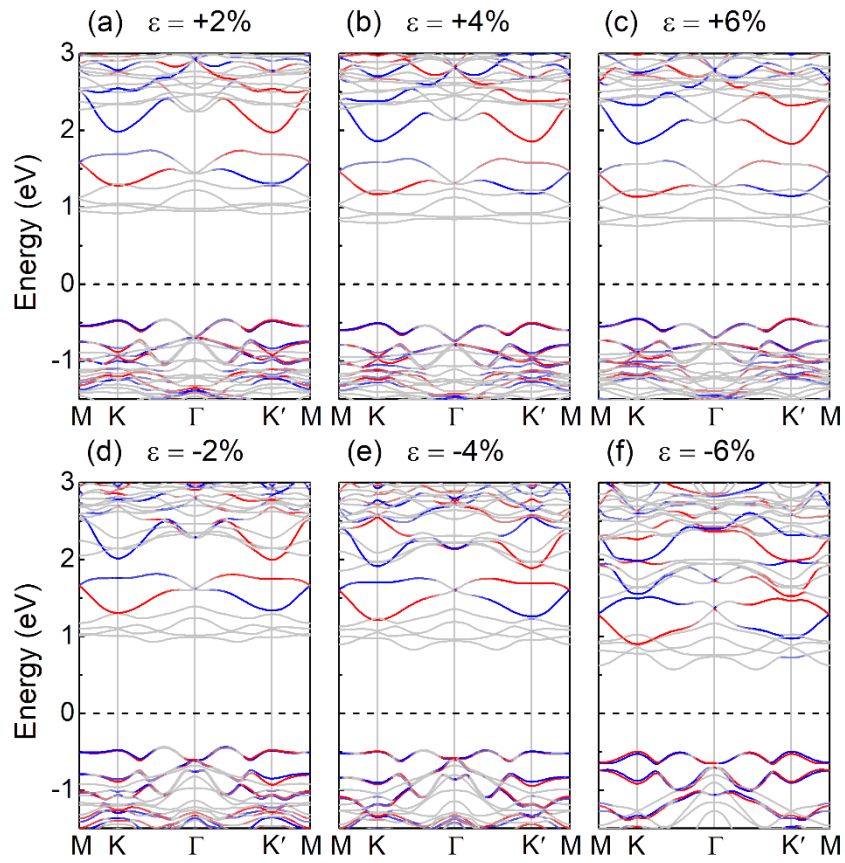


**Fig. S5** Band structures of  $\text{AgBiP}_2\text{S}_6/\text{CrBr}_3$  heterostructure in the polarized state P- under different strain from  $-6\%$  to  $+6\%$ . The Fermi level is set to zero.